

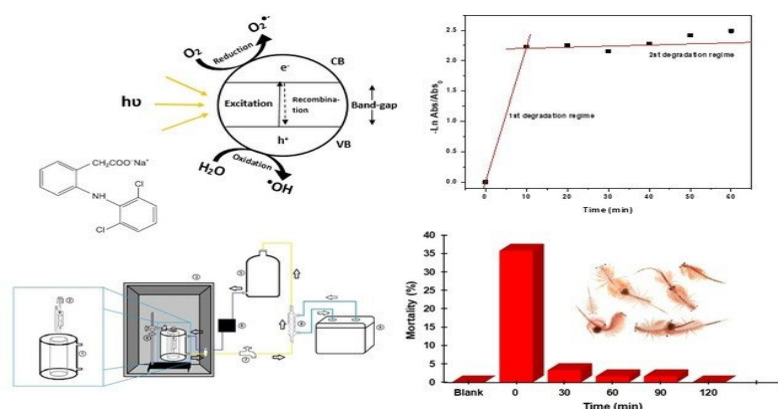
Full Paper | <http://dx.doi.org/10.17807/orbital.v14i4.17652>

Determination of the Heterogeneous Photodegradation Velocity Constant of Sodium Diclofenac with the Evaluation of Residual Toxicity in *Artemia salina*

Danilo Rodrigues de Souza ^a, Marcelo Galdino ^a, and Letícia da Silva Lima*^a

With population growth and increasing urbanization, pollution of aquatic matrices has become frequent, with many studies focused on emerging contaminants as they are recalcitrant and bioaccumulative substances. With the deficiency in conventional water and sewage treatments, this work seeks alternatives for the mitigation of these pollutants, proposing the role of heterogeneous photocatalysis in the degradation of drugs, in this case, sodium diclofenac (SDF). Photocatalytic tests were performed using a bench system. The samples obtained were quantified using a colorimetric method with the aid of a UV-Vis spectrophotometer. The main observation was intense and rapid degradation of the drug in the first 10 min, indicating a reduction in the concentration of 71.05%. For the periods of 0-10 min and 10-60 min, two photodegradation regimes were estimated, with the first regime having an apparent rate constant of 0.12394 min^{-1} and the second of 0.01601 min^{-1} . Toxicity bioassays were performed with the aid of *Artemia salina*, determining a 50% lethal concentration of $4.45 \times 10^{-4} \text{ mol L}^{-1}$. When performing a new photocatalysis to determine the toxicity of the waste generated it was possible to observe a significant decrease in toxicity in the first 30 min, reaching a total reduction in 120 min.

Graphical abstract



Keywords

Artemia salina
Emerging contaminants
Heterogeneous photocatalysis
Kinetics
Sodium diclofenac
Toxicity

Article history

Received 16 Aug 2021
Revised 10 Feb 2022
Accepted 26 Nov 2022
Available online 27 Dec 2022

Handling Editor: Adilson Beatriz

1. Introduction

The population growth is of the main causes of increased pollution in the world [1]. Studies indicate that a growth rate of the world population will increase in the coming years, reaching a total of 8.5 billion inhabitants in 2030 [2]. With this

phenomenon, some social events can be observed, how a greater urbanization, estimated that, in 2050, about 66% of the world population will be living in urban areas [3], implying a greater water contamination, due to exceeding handling of

^a Universidade Federal do Oeste da Bahia (UFOP). Rua da Prainha, 1326, zip code 47810-059, Barreiras, Bahia, Brazil. *Corresponding author. E-mail: danilo.souza@ufob.edu.br

different substances by the population, compromising its quality [4].

Studies involving the analysis of aquatic matrices, in large part, have been directed toward estimating the presence of emerging contaminants [5]. The term “emerging” define this pollutants as compounds with low occurrence, reported recently, or as compounds known with toxicological activities little understood, putting at risk the human health [5, 6]. Having great resistance in the environment and being present in several products, as pesticides, flame retardants, personal care products, drugs and among others [6], many researches have been accomplished, totalizing, in the period of 2000-2019, 4968 publications [7].

Among the studies carried out in this period, the drugs are the contaminants of greatest interest in the scientific world [7]. With complex contamination route, researches came to the conclusion that the largest of pharmaceutical products, in the aquatic matrices, occurs through the sewage system through the non-metabolized compounds excreted by humans [8]. However, when arriving at the treatment plants, such substances are not completely mitigated due to their high chemical and biological stability [9, 10].

The category that draws the most attention, between drugs, are non-steroidal anti-inflammatory drugs, being the diclofenac the most popular medicine in this class, marketed freely in most countries, with an estimated annual consumption of around 940 tonnes [11]. Studies prove, through the monitoring the concentration present, its occurrence in different aquatic environments of several countries [12], evidencing its presence in Brazilian rivers [13, 14]. Considered a bioaccumulative medicine, the diclofenac is characterized as a high priority drug from an ecotoxicological point of view [15], being present, since 2012, in “list of priority substances in the field of water policy” of the European Union [16], being determined, by the standard of environmental quality, a maximum permitted concentration this drug in the range of ngL^{-1} for fresh and marine waters [11].

In its turn, the treatment plants have a low efficiency when it comes to drugs decontamination. Not being designed for such purposes and with the main objective of elimination of the pathogenic agents, the traditional treatments only favor the reduction of the degradability of pharmaceutical compounds [17], being proven the presence of these contaminants in Brazilian treatment plants or in aquatic biotas close to them, indicating a potential threat [18, 19]. Thus, it is evident that these pollutants return to the environment, presenting occurrence in drinking water [20-22], causing serious impacts to the population [23].

The degradation of drugs in wastewater is indispensable for the availability of the water for consumption and, since the conventional treatments are not efficient, the use of more modern techniques is necessary [17]. Advanced oxidative processes (AOP) are being the focus of researchers, showing promising results with the photocatalysis, highlighting the photocatalytic properties of semiconductors, which are related to heterogeneous photocatalysis [24], considered a technology of great potential for the treatment of water [25]. This method consists in the use of a semiconductor that, in the presence of light, promotes the excitation of its electrons and, by means of oxidation reactions, produces radical species with high reactivity on its surface [26]. Once the reaction occurs in an aqueous medium, the photodegradation process promotes water dissociation, forming the radicals $\cdot\text{OH}$ [27] and, when the contaminant is adsorbed on the surface of the semiconductor material, it can be degraded by

the radicals present and the residues generated can be desorbed or remain on the surface until they are transferred to the fluid under treatment [28], Fig. 1.

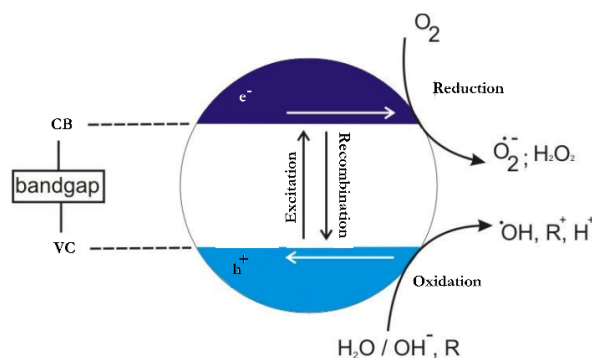


Fig. 1. Schematic representation of the radical production process oxidants from a TiO_2 particle in a solution (adapted) [29, 30].

The heterogeneous photocatalysis is already used in countless works in the degradation of drugs, using, as a semiconductor in the photodegradation process, the TiO_2 [29, 30]. Studies focused on the mineralization of diclofenac using this technique have also been performed, proving its efficiency [31-33], however, it's necessary the realization of toxicity bioassays of the waste generated, since they are fundamental for the determination of the toxic character of the fluid after treatment [34].

When it comes to drugs, the by-products formed in the degradation can favor an increase in toxicity, as evidenced by Huong Le in the initial degradation of the drug acetaminophen by means of AOP [35], and, studies demonstrate that the metabolites formed in the treatment of residues, containing diclofenac, are more toxic than the substance itself in its original form [11]. However, since phototransformation processes can achieve high levels of oxidation with the formation of highly active radicals [36], these are capable of to come up with an almost complete degradation, eliminating the by-products formed and, consequently, reducing the toxicity of the fluid. Therefore, it is evident the necessity for biological tests for the monitoring of the waste that will be released, following its behavior after the treatment in order to keep the stability of the environment [17].

In this study, we report the behavior of sodium diclofenac (SDF), determining its photodegradation kinetics when exposed to the heterogeneous photocatalysis process, using TiO_2 as a semiconductor, in addition to the application of the residue obtained, after treatment, in a bioassay with *Artemia salina*, checking if there was a reduction of the toxicity.

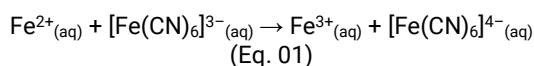
2. Results and Discussion

2.1. Construction of the calibration curve for determination of sodium diclofenac

The standard sample of sodium diclofenac was analyzed in the UV-Vis spectrophotometer verifying the maximum absorption of the substance at 275 nm (Fig. 2).

In order to move this absorption to the region of visible light, an oxidation reaction is conducted between iron (III) chloride and sodium diclofenac, wherein this last one favors the reduction of the former, promoting the transformation of

Fe^{3+} to Fe^{2+} , and this cation, in turn, reacts with potassium ferricyanide (Equation 1) [37].



The reaction proceeds to the formation the $\text{Fe}_4[\text{Fe}(\text{CN})_6]_3$ complex (Equation 02), also known as Prussian blue for its bluish coloring [38].

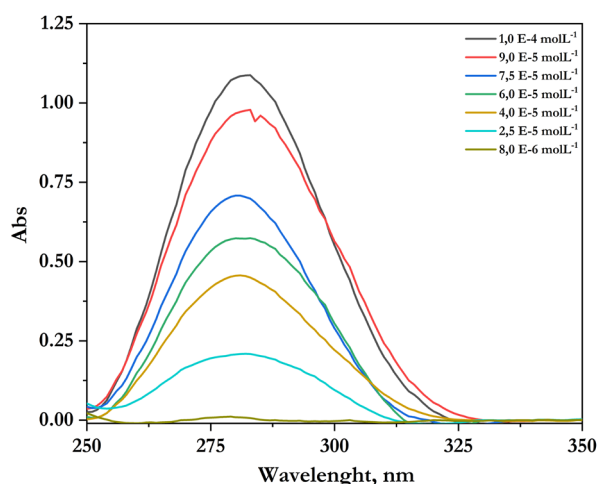
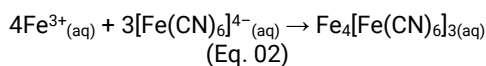


Fig. 2. Scanning of standard sodium diclofenac samples (250 – 350 nm).

With the blue solution, it is then possible to obtain measurements in the wavelength range between 400-800 nm and still estimate the concentration of sodium diclofenac in an indirect way, since its concentration is proportional to the concentration of Prussian blue. The scanning measurements obtained in the spectrophotometer of the sodium diclofenac solutions after the formation of the complex are shown in Fig. 3.

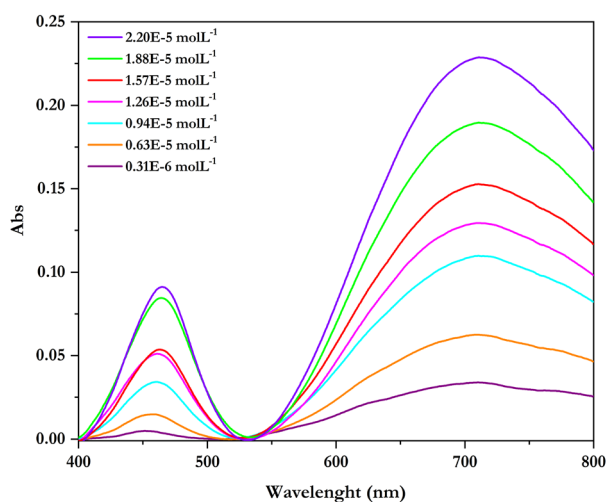


Fig. 3. Scanning of sodium diclofenac solutions at concentrations from 1 to 7 mgL^{-1} , after a reactional process of iron complexation, in the range 400 to 800 nm, with $\lambda_{\text{m}\ddot{\text{a}}\text{x}} = 720$ nm.

Analyzing the spectrum of the solutions, it is possible to identify a maximum absorption wavelength ($\lambda_{\text{m}\ddot{\text{a}}\text{x}}$) in common,

having a value of 720 nm and, from there, construct the calibration curve (Fig. 4).

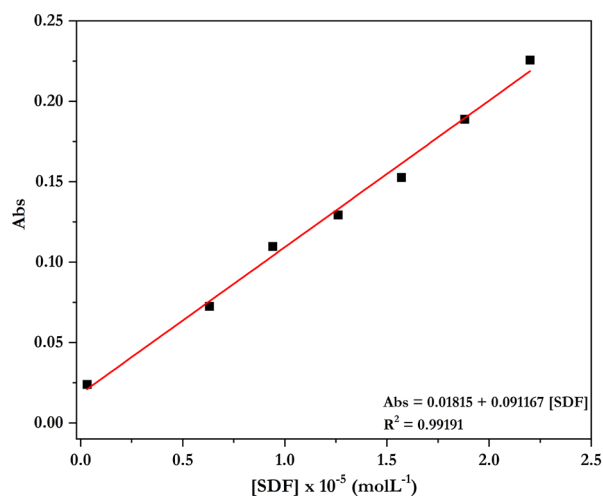


Fig. 4. Calibration curve obtained after scanning data in the spectrophotometer of solutions with different concentrations of sodium diclofenac after the formation of Prussian blue.

The obtained curve had a coefficient of determination (R^2) of 0.99191, indicating that its adjustment to the linear model is adequate with the obtained values. The detection limit of $0.661 \times 10^{-5} \text{ molL}^{-1}$ and a quantification limit of $1.99 \times 10^{-5} \text{ molL}^{-1}$.

2.2 Photodegradation kinetics

The analyzes in spectrophotometer were performed for each sample collected in their respective time, being possible to observe the reduction of the concentration of diclofenac with the progress of photodegradation through the reduction of the absorbance intensity (Fig. 5).

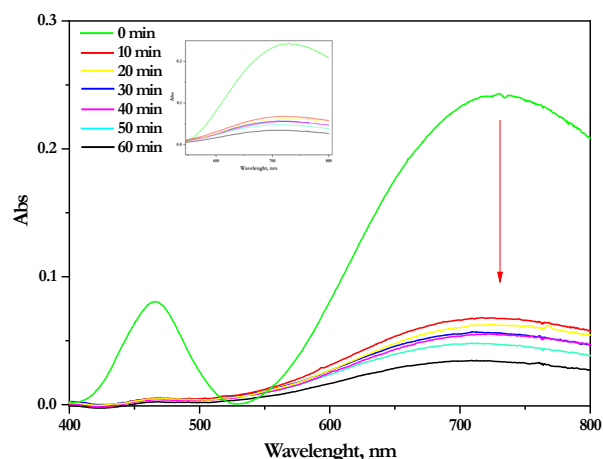


Fig. 5. Samples collected every 10 min between 0 and 60 min of the sodium diclofenac photodegradation process.

The wavelength adopted was 720 nm, obtaining the mean of absorbance (Abs) and estimating the concentration of sodium diclofenac, in each sample, applying the Abs value in the line equation obtained through the calibration curve (Table 1).

Table 1. Mean absorbance of the samples collected in their respective times and the estimated concentrations of sodium diclofenac (SDF) present.

Time (min)	Abs	[SDF] x 10 ⁻⁵ (molL ⁻¹)
0	0.26116	2.67
10	0.07562	0.63
20	0.06243	0.49
30	0.05613	0.42
40	0.04994	0.35
50	0.04167	0.26
60	0.03216	0.15

The oxidative photodegradation reaction occurs in an steady-state, keeping a high concentration of hydroxyl radicals in the reaction medium [39], which, when incorporated into the diclofenac molecule, competes for the electrons present, causing the disruption of drug bonds and, consequently, their degradation [40]–[42]. Taking into consideration that the quantity of sodium diclofenac is much smaller compared to the concentration of the $\cdot\text{OH}$ radical produced, one can consider that the latter remains constant during the degradation process [39]. The rate equation given by $v = k[\text{SDF}][\cdot\text{OH}]$, Where in [SDF] corresponds to the concentration of diclofenac and $[\cdot\text{OH}]_0$ the initial concentration of the hydroxyl radical, can be rewritten as $v = k_{\text{app}} [\text{SDF}]$, Where, $k_{\text{app}} = k[\cdot\text{OH}]$, getting a pseudo-first order kinetic [43].

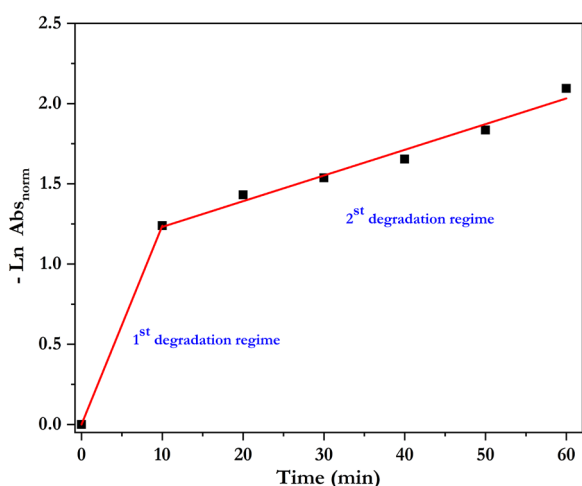
The speed law of the pseudo-first order kinetic is integrated in order to obtain a relation between the concentration of diclofenac present in the photocatalytic process in function of time, obtaining Equation 03:

$$\ln \frac{[\text{SDF}]_t}{[\text{SDF}]_0} = -k_{\text{app}} t \quad (\text{Eq. 03})$$

being able to estimate the apparent rate constant (k_{app}). Since the concentration of the pollutant to be degraded is equivalent to the absorbance obtained after analysis of each sample at that time, a correlation can be constructed (Equation 04):

$$\ln \frac{\text{Abs}_t}{\text{Abs}_0} = \ln \frac{[\text{SDF}]_t}{[\text{SDF}]_0} \quad (\text{Eq. 04})$$

in function of the collection time, obtaining the reaction kinetics graph (Fig. 6).

**Fig. 6.** Study of the photodegradation kinetics of sodium diclofenac in 60 min. It is possible to observe the formation of two degradation regimes, in which, each one presents different apparent rate constants (k_{app}).

With the construction of the graph, it was possible to observe a accented decrease in the concentration of sodium

diclofenac in the first 10 min, evidencing the presence of two reactional regimes, the first being in the period from 0 to 10 minutes, whose equation is $y = 7.8504 \times 10^{-17} + 0.12394x$, and the second in the period of 10 to 60 minutes, whose equation is $y = 1.07154 + 0.01601x$. Through the line equation obtained in each regime, it was possible to estimate the velocity constants referring to them, obtaining the value of 0.12394 min^{-1} for the first degradation regime and the value of 0.01601 min^{-1} for the second degradation regime.

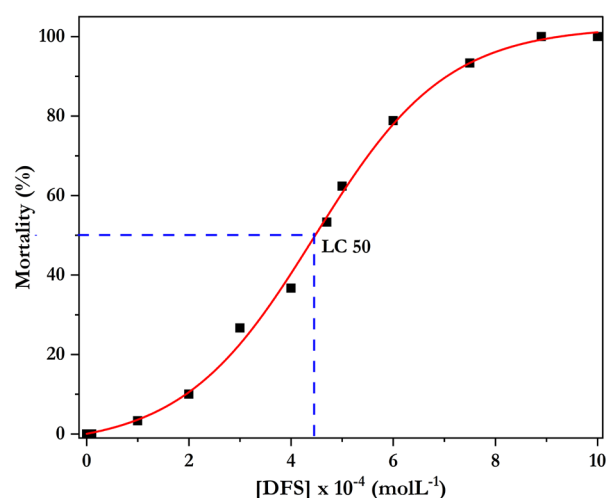
The two apparent velocity constants differ in 7.74 times, proving that the first regime occurred at a higher velocity compared to the second. The total photodegradation reached 88.1%. In 10 minutes of photocatalytic process, the concentration of sodium diclofenac fell in 71.05 %, while in the remaining 50 minutes; the concentration just decayed 10.05%, evidencing the influence of the concentration, because, in higher concentrations, degradation occurs in higher speeds.

2.3 Determination of Lethal Concentration in 50% (LC 50)

After 48 hours of exposure, the survivors *Artemia salina* were counted, obtaining their value for each concentration of sodium diclofenac used. In Table 2, the mean of the survival of each sample made in triplicate is presented, as well as its standard deviation, being possible to convert the survival response signal to the mortality in percentage.

Table 2. Mean survival of *Artemia salina* after 48 hours of exposure to sodium diclofenac, with its standard deviation and mortality, for each concentration, in percentage.

[SDF] x 10 ⁻⁴ (molL ⁻¹)	Mean	SD	Mortality (%)
0	10.00	0.00	0.00
0.01	10.00	0.00	0.00
0.1	10.00	0.00	0.00
1.0	9.67	0.51	3.33
2.0	9.00	0.00	10.00
3.0	5.67	0.57	26.66
4.0	6.33	0.57	36.67
4.7	4.67	0.52	53.30
5.0	3.00	0.00	62.33
7.5	0.67	0.50	93.33
8.9	0.00	0.00	100.00
10.0	0.00	0.00	100.00

**Fig. 7.** Determination of the lethal concentration for 50% of the living species through of the mortality measures for the different concentrations of sodium diclofenac. The value obtained, as marked in the graph, was $4.41 \times 10^{-4} \text{ molL}^{-1}$.

With the mortality of each concentration, it was possible to construct the graph to determine the lethal concentration for 50% of the living species (LC50) (Fig. 7).

The obtained sigmoid curve determines the lethal concentration (LC) for the mortality of 50% of the species used for monitoring. Through the graph, a concentration of $4.45 \times 10^{-4} \text{ mol L}^{-1}$ was obtained, determinant for the death of half of the microcrustaceans present in the sample. This result is significant for new toxicity tests.

2.4 Bioassay of waste generated after photodegradation process

After the exposure for the period of 48 hours to the residue resulting from the photodegradation process of sodium diclofenac, the surviving *Artemia salina* were quantified in each sample collected in its referred time (Table 3).

Table 3. Mortality reduction of the *Artemia salina* exposed to diclofenac sodium samples after photocatalytic treatment.

Photo-degradation time (min)	[SDF] $\times 10^{-3}$ (mol L^{-1})	Mean	SD	Mortality (%)
0	1.0130	6.43	0.23	35.71
30	0.1560	9.45	0.51	5.49
60	0.1153	9.59	0.38	4.06
90	0.0863	9.69	0.41	3.04
120	0.0445	10.00	0.00	0.00

From the data obtained, it is possible to obtain a graph of the mortality of *Artemia salina* in function of the time of treatment by photodegradation (Fig. 8).

The reference measures of the blank found that only the presence of the photocatalytic residue contributed to the mortality of *Artemia salina*, being possible to observe a decrease in mortality with the increase of the permanence time of the residue in the photocatalytic process, with this getting at 0% in time of 120 min. Correlating the results obtained expressed in Figure 8 with the values of the concentrations of diclofenac sodium after its photodegradation, presented in Table 3, it can be inferred that, with the increase of reactional time, the sodium diclofenac has a highest index of degradation, reducing the toxicity of the residues formed, for *Artemia salina*, in 100%.

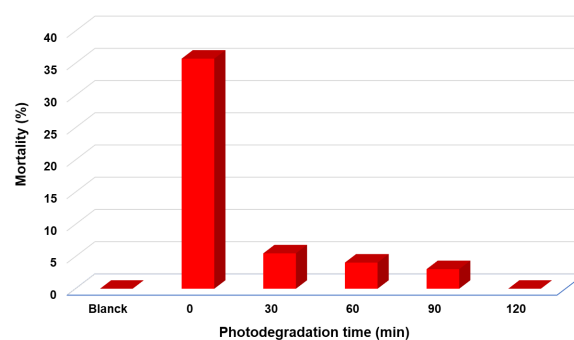


Fig. 8. Graph relating the mortality rate of *Artemia salina* for each sample collected in their respective time during the photodegradation process of sodium diclofenac. It is possible to observe a decrease in mortality the longer the sample remains.

3. Material and Methods

3.1 Materials

TiO₂ (Evonik Degussa P25) without previous treatment. Hydrochloric acid (Synth – 36.5 – 38.0%), potassium ferricyanide (Synth – 99.0%), iron (III) chloride (Dinâmica – 97.0 – 102.0%). Sodium diclofenac (Pharmanostra – 99.18%) obtained in a handling pharmacy. Sea salt and *Artemia salina* eggs, commercially obtained.

3.2 Instruments

A photocatalytic system composed for a wooden box containing a medium pressure mercury vapor lamp (400 W) and a glass reactor, connected to the hoses (with a collection tap) and a cooling system (Fig. 9).

For the filtration of the collected samples, a support for the filtration of 13 mm Millipore/Swinnex and filter papers with porosity of 0.2 μm were used. The presence of diclofenac was detected using a Varian/Cary 50 Probe spectrophotometer. The incubation of *Artemia salina* was done in a system composed of a glass aquarium with a connected pump, for aeration of the medium, and a light fixture containing a fluorescent lamp as a light source for the eggs to hatch, all commercially obtained (Fig. 10).

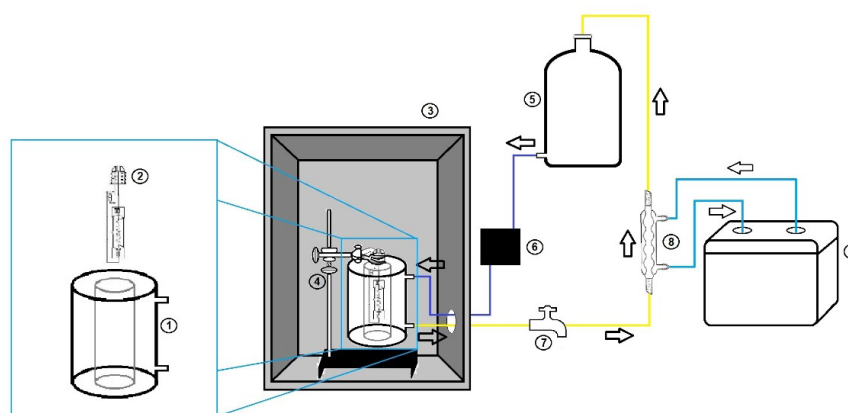


Fig. 9. Complete photocatalytic system composed of a photocatalytic reactor (1) and a Mercury Vapor lamp (2) that are inside a properly isolated wooden box (3) on a universal support (4). The solution is inserted into the system through the Mariotte bottle (5) and pumped through it by means of the circulation electric pump (6) with a tap for collecting samples (7). The cooling occurs in external midst inside the condenser (8) by means of water that is cooled in the cooling reservoir (9).

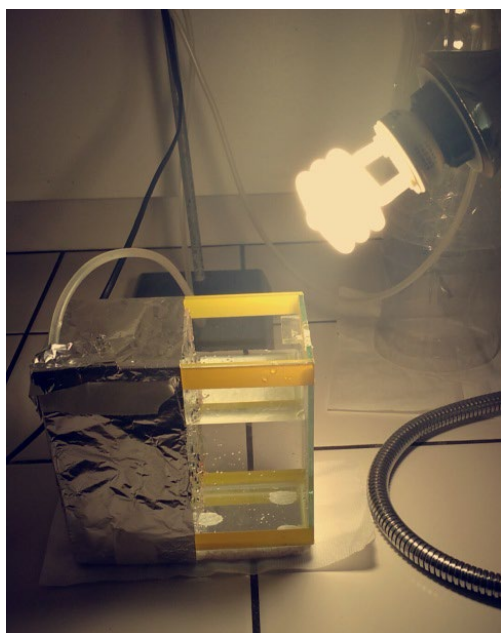


Fig. 10. System for hatching the cysts. The aquarium is divided, having a partially isolated side from the light, by an acrylic plate containing small holes for the passage of the *Artemia salina* after hatching to the fully illuminated side.

3.3 Methods

3.3.1 Construction of the calibration curve

This methodology was based on Mahood and Hamezh [37]. Stock solutions of iron (III) chloride, potassium ferricyanide and sodium diclofenac were prepared, with concentrations of $3.0 \times 10^{-2} \text{ molL}^{-1}$, $1.0 \times 10^{-3} \text{ molL}^{-1}$ and $1.57 \times 10^{-4} \text{ molL}^{-1}$, respectively, with the addition 1.0 ml of hydrochloric acid concentrated in the iron (III) chloride solution. The analysis solutions were prepared from 1.5 ml of the iron (III) chloride solution and 1.0 ml of the potassium ferricyanide solution, with different aliquots of the sodium diclofenac stock solution to obtain the concentrations of 3.14×10^{-6} to $2.20 \times 10^{-5} \text{ molL}^{-1}$ (1 to 7 mgL^{-1}), with a final volume of 25 ml, waiting 20 min for its stabilization. The solutions were analyzed on the spectrophotometer by the slow speed scanning method until the wavelength of 800 nm.

3.3.2 Heterogeneous photocatalysis

In the photocatalytic system, 4 L of sodium diclofenac solution with a concentration of 50 mgL^{-1} ($1.57 \times 10^{-4} \text{ molL}^{-1}$) and 0.4 g (0.1 gL^{-1}) of titanium dioxide are added. The pH is measured at approximately 3.0. After these adjustments, the Hg vapor lamp is turned on, waiting 5 minutes for stabilization of the irradiation, after that, the photocatalytic process begins. The initial sample (0 min) is collected, and the others samples, every 10 minutes until to reach 60 min. All samples were filtered properly. To monitor the concentration of sodium diclofenac in the samples collected, the Mahood and Hamezh methodology is also used [37]. A aliquot of 3 ml of each sample is used to prepare 25 ml solutions, containing 1.5 ml of iron (III) chloride solution and 1.0 ml of potassium ferricyanide solution. After 20 min, the samples were analyzed, in triplicate, in the spectrophotometer, using the same specifications of the calibration curve.

3.3.3 Toxicity monitoring

3.3.3.1 Determination of Lethal Concentration in 50% (LC_{50})

The cysts of *Artemia salina* were incubated in an aquarium containing a 20 gL^{-1} saline solution, being illuminated for 48 hours. After the hatching, the Artemias were exposed to different sodium diclofenac solutions using saline solution as solvent, with concentrations of 1×10^{-10} , 1×10^{-8} , 1×10^{-6} , 1×10^{-5} , 1×10^{-4} , 2×10^{-4} , 3×10^{-4} , 4×10^{-4} , 4.7×10^{-4} , 5×10^{-4} , 7.5×10^{-4} , 8.9×10^{-4} , $1 \times 10^{-3} \text{ molL}^{-1}$, in addition to blank solution (saline without adding diclofenac) to be used as a reference. For each solution, a triplicate was performed, containing 10 units of *Artemia salina* in each. After the period of 48 hours exposed under the light from the fluorescent lamp, the number of survivors were counted.

3.3.3.2 Bioassay of waste generated after photodegradation process

After estimating the LC_{50} , a photodegradation process was performed using a sodium diclofenac solution with 300 mgL^{-1} ($1.013 \times 10^{-3} \text{ molL}^{-1}$) concentration, and the same settings applied in topic 3.3.2. Aliquots of 16.7 mL were collected and filtered of the waste generated, at 0, 30, 60, 90 and 120 minutes, for the preparation of the solutions, using saline water as a solvent, obtaining a final volume of 100 mL. For each solution of their respective photodegradation time, a triplicate was made containing 10 units of *Artemia salina* in each one, in addition to the presence of blank solution for reference. After 48 hours exposed to constant light, they were quantified.

4. Conclusions

The colorimetric method, which produces the Prussian blue compound, was very effective for the determination of sodium diclofenac, favoring the obtaining of a calibration curve with R^2 of 0.99191, making it possible to determine the concentration of the drug after its photodegradation. The absorbance results, after the heterogeneous photocatalysis process, demonstrate a great efficiency in the degradation of sodium diclofenac, with an accelerated reduction of its concentration in the first 10 min of the process, obtaining a velocity constant of 0.12394 min^{-1} for this regime, being 7.74 times greater than the second regimen that occurred between 10 and 60 min, with a total reduction of 88.1% of the drug molecule in the medium. With the obtaining of the LC_{50} of $4.45 \times 10^{-4} \text{ molL}^{-1}$, it was possible to obtain the results of toxicity for the photodegraded samples, observing a behavior pattern to the verify the reduction of toxicity in a drastic way in the first minutes of the oxidative process advanced, reaching 5.49% mortality in the first 30 min and 0% mortality with 120 min. It is evident, thus, that the heterogeneous photocatalysis process, with the configurations adopted in this work, enabled the degradation of the drug sodium diclofenac, in addition to reducing its toxicity, demonstrating its potential for application in water and sewage treatment plants, be in the pre or after treatment of the effluent.

Acknowledgments

To Universidade Federal do Oeste da Bahia – UFOB (CT-INFRA 01/2013: convenio 01.14.0137.00), to Universidade Federal de Uberlândia – UFU (FINEP INFR13 01.13.0371.00), CAPES, CNPq, Evonik Brasil and Research Group on Materials Sciences and Photocatalysis (CMFOT).

Author Contributions

Letícia da Silva Lima (Conceptualization, Data Curation, Formal Analysis, Investigation, Methodology, Validation, Visualization, Writing – original draft, Writing – review & editing); Danilo Rodrigues de Souza (Conceptualization, Funding Acquisition, Methodology, Project Administration, Resources, Writing and Supervision); Marcelo Marinho Galdino (Conceptualization, Data Curation, Formal Analysis, Investigation, Methodology, Validation).

References and Notes

- [1] Alam, M. M.; Murad, M. W.; Noman, A. H. M.; Ozturk, I. *Ecol. Indic.* **2016**, *70*, 466. [\[Crossref\]](#)
- [2] United Nations, Department of Economic and Social Affairs, Population Division (2015). World Population Prospects: The 2015 Revision, Key Findings and Advance Tables. Working Paper No. ESA/P/WP.241.
- [3] Jensen, O.; Wu, H. *Environ. Sci. Policy* **2018**, *83*, 33. [\[Crossref\]](#)
- [4] Peña-Guzmán, C. et al. *J. Environ. Manage* **2019**, *237*, 408. [\[Crossref\]](#)
- [5] Sutherland, D. L.; Ralph, P. J. *Water Res.* **2019**, *164*, 14921. [\[Crossref\]](#)
- [6] Álvarez-Ruiz, R.; Picó, Y. *Trends Environ. Anal. Chem.* **2020**, *25*. [\[Crossref\]](#)
- [7] Ramírez-Malule, H.; Quiñones-Murillo, D. H.; Manotas-Duque, D. *Emerg. Contam.* **2020**, *6*, 179. [\[Crossref\]](#)
- [8] Wilkinson, J.; Hooda, P. S.; Barker, J.; Barton, S.; Swinden J. *Environ. Pollut.* **2017**, *231*, 954. [\[Crossref\]](#)
- [9] Benedetti, B. et al. *Microchem. J.* **2020**, *155*. [\[Crossref\]](#)
- [10] Krzeminski, P. et al. *Sci. Total Environ.* **2019**, *648*, 1052. [\[Crossref\]](#)
- [11] Lonappan, L.; Brar, S. K.; Das, R. K.; Verma, M.; Surampalli, R. Y. *Environ. Int.* **2016**, *96*, 127. [\[Crossref\]](#)
- [12] Sathishkumar, P.; Meena, R. A. A.; Palanisami, T.; Ashokkumar, V.; Palvannan, T.; Gu, F. L. *Sci. Total Environ.* **2020**, *698*, 134057. [\[Crossref\]](#)
- [13] de Sousa, D. N. R.; Mozeto, A. A.; Carneiro, R. L.; Fadini, P. S. *Environ. Sci. Pollut. Res.* **2018**, *25*, 4607. [\[Crossref\]](#)
- [14] Pereira, C. D. S. et al. *Sci. Total Environ.* **2016**, *548-549*, 148. [\[Crossref\]](#)
- [15] Li, Y.; Zhang, L.; Liu, X.; Ding, J. *Sci. Total Environ.* **2019**, *658*, 333. [\[Crossref\]](#)
- [16] Carvalho, R. N.; Ceriani, L.; Ippolito, A. Development of the first Watch List under the Environmental Quality Standards Directive water policy. EUR 27142. Luxembourg (Luxembourg): Publications Office of the European Union; 2015. JRC95018. [\[Crossref\]](#)
- [17] Kaur, A.; Umar, a.; Kansal, S. K. *Appl. Catal. A Gen.* **2016**, *510*, 134. [\[Crossref\]](#)
- [18] Chaves, M. J. S. et al. *Sci. Total Environ.* **2020**, *734*, 139374. [\[Crossref\]](#)
- [19] Pivetta, R. C.; Rodrigues-Silva, C.; Ribeiro, A. R.; Rath, S. *Sci. Total Environ.* **2020**, *727*, 138661. [\[Crossref\]](#)
- [20] Baken, K. A.; Sjerps, R. M. A.; Schriks, M.; van Wezel, A. P. *Environ. Int.* **2018**, *118*, 293. [\[Crossref\]](#)
- [21] Riva, F.; Castiglioni, S.; Fattore, E.; Manenti, A.; Davoli, E.; Zuccato, E. *Int. J. Hyg. Environ. Health* **2018**, *221*, 451. [\[Crossref\]](#)
- [22] Sharma, B. M. et al. *Sci. Total Environ.* **2019**, *646*, 1459. [\[Crossref\]](#)
- [23] Medina Amado, C.; Minahk, C. J.; Cilli, E.; Oliveira, R. G.; Dupuy, F. G. *Biochim. Biophys. Acta - Biomembr.* **2020**, *1862*, 183135. [\[Crossref\]](#)
- [24] Rueda-Marquez, J. J.; Levchuk, I.; Fernández Ibañez, P.; Sillanpää, M. *J. Clean. Prod.* **2020**, *258*. [\[Crossref\]](#)
- [25] Wetchakun, K.; Wetchakun, N.; Sakulsermsuk, S. *J. Ind. Eng. Chem.* **2019**, *71*, 19. [\[Crossref\]](#)
- [26] Al-Mamun, M. R.; Kader, S.; Islam, M. S.; Khan, M. Z. H. *J. Environ. Chem. Eng.* **2019**, *7*, 103248. [\[Crossref\]](#)
- [27] Guo, Q.; Zhou, C.; Ma, Z.; Yang, X. *Adv. Mater.* **2019**, *31*, 1. [\[Crossref\]](#)
- [28] Gopinath, K. P.; Madhav, N. V.; Krishnan, A.; Malolan, R.; Rangarajan, G. *J. Environ. Manage* **2020**, *270*, 110906. [\[Crossref\]](#)
- [29] Awfa, D.; Ateia, M.; Fujii, M.; Johnson, M. S.; Yoshimura, C. *Water Res.* **2018**, *142*, 26. [\[Crossref\]](#)
- [30] Varma, K. S.; Tayade, R. J.; Shah, K. J.; Joshi, P. A.; Shukla, A. D.; Gandhi, V. G. *Water-Energy Nexus* **2020**, *3*, 46. [\[Crossref\]](#)
- [31] Mugunthan, E.; Saidutta, M. B.; Jagadeeshbabu, P. E. *Environ. Nanotechnology, Monit. Manag.* **2018**, *10*, 322. [\[Crossref\]](#)
- [32] Apopei, P. et al. *Process Saf. Environ. Prot.* **2020**, *138*, 324. [\[Crossref\]](#)
- [33] Nguyen, C. H.; Tran, M. L.; Van Tran, T. T.; Juang, R. S. *Sep. Purif. Technol.* **2020**, *232*, 115962. [\[Crossref\]](#)
- [34] Hong, M.; Wang, Y.; Lu, G. *Chemosphere* **2020**, *127351*. [\[Crossref\]](#)
- [35] Le, T. X. H. et al. *Chemosphere* **2017**, *172*, 1. [\[Crossref\]](#)
- [36] Niu, L. et al. *J. Environ. Sci. (China)* **2020**, *96*, 109. [\[Crossref\]](#)
- [37] Barry, A.; Mahood, M.; JHamezh, M. *J. Kerbala Univ.* **2009**, *7*, 310.
- [38] Busquets, M. A.; Estelrich, J. *Drug Discov. Today* **2020**, *25*, 1431. [\[Crossref\]](#)
- [39] Schneider, J. et al. *Chem. Rev.* **2014**, *114*, 9919. [\[Crossref\]](#)
- [40] Wang, F. et al. *Chem. Eng. J.* **2019**, *356*, 857. [\[Crossref\]](#)
- [41] Liu, D. et al. *Chem. Eng. J.* **2019**, *369*, 968. [\[Crossref\]](#)
- [42] Irandost, M.; Akbarzadeh, R.; Pirsaeheb, M.; Asadi, A.; Mohammadi, P.; Sillanpää, M. *J. Mol. Liq.* **2019**, *291*, 111342. [\[Crossref\]](#)
- [43] Simonin, J. P. *Chem. Eng. J.* **2016**, *300*, 254. [\[Crossref\]](#)

How to cite this article

de Souza, D. R.; Gladino, M.; Lima, L. S. *Orbital: Electron. J. Chem.* **2022**, *14*, 221. DOI: <http://dx.doi.org/10.17807/orbital.v14i4.17652>